Accident Analysis and Prevention 132 (2019) 105283

Contents lists available at ScienceDirect

Accident Analysis and Prevention

journal homepage: www.elsevier.com/locate/aap

Incorporating spatial effects into temporal dynamic of road traffic fatality risks: A case study on 48 lower states of the United States, 1975–2015

Hanchu Zhou[a], Helai Huang[a,*], Pengpeng Xu[b], Fangrong Chang[a], Mohamed Abdel-Aty[c]

[a] School of Traffic and Transportation Engineering, Central South University, Changsha, Hunan, China
[b] Department of Civil Engineering, The University of Hong Kong, Pokfulam Road, Hong Kong, China
[c] Department of Civil, Environmental, and Construction Engineering, University of Central Florida, Orlando, FL 32816, United States

ARTICLE INFO

Keywords:
Traffic fatality risks
Temporal dynamics
Spatial correlation
Spatial Markov chains

ABSTRACT

The rate of road traffic fatalities has long served as a regular indicator to evaluate and compare road safety performance for different administrative divisions. This article introduces a novel method known as the Markov chain spatial model to incorporate the spatial effects into the temporal dynamic of the fatality rates. Compared to the traditional Markov chain model, the proposed spatial Markov chain model can quantify the influence of neighboring sites explicitly in the transition process. A case study using a long duration dataset, from 1975 to 2015 in the 48 lower states of the United Sates, was conducted to illustrate the proposed model. The fatality rates were measured as the number of traffic fatalities per 100 million vehicle miles or per 10,000 residents. The results show that the probability of transition for one state between different levels of traffic fatality risks depends largely on the context of its surrounding neighbors. Another important finding is that relative to the estimates of traditional Markov chain models, states surrounded by neighborhoods with relatively low fatality rates take a longer time to transform to a higher level of fatality risk in the spatial Markov chain model. On the other hand, those with high-risk neighborhoods takes less time to deteriorate. These findings confirm that it is imperative to incorporate spatial effects when modeling the temporal dynamic of safety indicators to assess and monitor the safety trends in the areas of interest.

1. Introduction

According to the World Health Organization, traffic crashes are one of the leading causes of death around the world (World Health Organization, 2015). It is important to understand, interpret, and forecast the trends of road safety and then implement appropriate countermeasures to prevent crash occurrence and reduce injury severity. For this purpose, traffic safety indicators, such as fatality risk and the number of injury crashes and victims, are regularly collected to monitor the safety trend of specific sites (Bergel-Hayat et al., 2013).

Time series methods are generally used in safety analyses to provide an initial insight into processes influencing road safety indicators over a regular time interval (e.g., year, quarter, or month) (Commandeur et al., 2013). Although the use of time series models are relatively scarce in traffic safety studies compared to the cross-sectional models (Lavrenz et al., 2018), several time series approaches have recently prevailed in traffic safety research, including the autoregressive integrated moving average models (ARIMA) (Quddus, 2008; Sebego et al., 2014), autoregressive conditional heteroscedasticity family models (ARCH family) (Ko and Guensler, 2004), generalized linear models (GLM) (Ahangari et al., 2016), structural equation models (SEM) (Bergel-Hayat et al., 2013), vector error correction models (VECM) (Bougueroua and Carnis, 2016; Li et al., 2018), frequency domain models (Boroujerdian et al., 2014), and state space models (Xu et al., 2019). Compared with aforementioned time-series models, Markov family models have a unique advantage because the safety indicator can change between several states over time by allowing the state variables to follow a stationary N-state Markov chain process in time, where the N-state means that the data are divided into N states and boundary of each state are constant during the whole Markov transition process (Malyshkina and Mannering, 2009; Malyshkina et al., 2009). Moreover, as noted by Gubner (2006), another reason for the popularity of the Markov chain theory used to capture the transitions of states is its simplicity with “memory-less” character which means Markov chain model can make predictions for the future of the process based solely on its present state.

* Corresponding author.
E-mail addresses: zhc0319@csu.edu.cn (H. Zhou), huanghelai@csu.edu.cn (H. Huang), pengpengxu@yeah.net (P. Xu), fangrongchang@csu.edu.cn (F. Chang), M.Aty@ucf.edu (M. Abdel-Aty).

https://doi.org/10.1016/j.aap.2019.105283
Received 28 November 2018; Received in revised form 17 August 2019; Accepted 25 August 2019
Available online 10 September 2019

Spatial analysis has become another essential topic in safety modeling in the past decade. Road safety indicators are usually aggregated over a macroscopic area, such as traffic analysis zones (Xu et al., 2014; Xu and Huang, 2015), census tracts (Abdel-Aty et al., 2013), counties (Huang et al., 2010), and states (Noland, 2003). Significant geographical association of crash statistics between adjacent spatial units has been widely found (Wang et al., 2012; Zeng and Huang, 2014; Lee et al., 2015; Huang et al., 2017; Xu et al., 2017). Considering that spatial effects may partially capture unobserved heterogeneity and provide the "pool strength" from neighboring sites, spatial effects, i.e., spatial dependence/correlation and spatial heterogeneity, have been comprehensively examined in numerous traffic safety analyses (Loo and Anderson, 2015).

A limited number of studies have recently investigated and confirmed the presence of space-time interactions based on various analytic units (Aguero-Valverde and Jovanis, 2006; Dong et al., 2016; Truong et al., 2016; Liu and Sharma, 2017; Meng et al., 2017; Liu and Sharma, 2018), which leads to a growing interest in studying the space-time variation. Almost all of the relevant studies used Bayesian conditional autoregressive (CAR) and its variations in spatio-temporal safety analysis, which can result in better model goodness of fit and more precise estimations. However, these studies investigated the space-time interactions based on an implicit assumption that the traffic safety state is stable during the whole study period, which has been doubted by several studies (Malyshkina et al., 2009; Park and Lord, 2009). Hence, the existence of spatial effects on historical safety state changing over time remains uncertain. Moreover, if the likelihood of a spatial unit to change its safety state in the future is influenced by its neighboring context, it is necessary to determine the strength of this influence. As such, the technique of spatial Markov chain is introduced in this study to model the safety state switching in terms of a spatial effect influences. This is an extension of the classic Markov chain by incorporating a spatial dimension to model the state transition process (Rey, 2001). By using the transition probability matrix of this model, the spatial effects on safety state switching can be evaluated and summarized directly.

This study aims to investigate whether, or not, there is a spatial effect on the changing pattern of safety state. Specifically, the purpose is to quantify the influence of an area's spatial features on its level of traffic fatality risk. Thus, this study attempts to model the diffusion of safety state over time at an aggregate level. It answers the question as to whether, or not, models that attempt to analyze traffic safety changing trends need to explicitly and accurately take spatial effects into account. The spatial Markov chains are applied to quantify the strength and duration of spatial effect on road safety dynamics since the aforementioned advantages. If the importance and significance of area location could be established, then there would be a strong motivation for safety experts to gain understandings of spatial effects. Furthermore, the results from this study can be used to help safety policymaking, especially provide supports when setting achievable long-term targets for road safety management departments. As the empirical example, two different kinds of fatality risk levels in the lower 48 states of the U.S. (i.e., 48 adjoining U.S. states, excluding the non-contiguous states of Alaska and Hawaii, District of Columbia and all off-shore insular areas) and the comparative spatial autoregressive (SAR) models were used to demonstrate the advances of using the spatial Markov chain model.

This paper is organized as follows. The following section introduces the analysis technique of classic and spatial Markov chains. Section 3 provides a description of the data used in this study: the fatality risk levels in the lower 48 states of the U.S. (i.e. 48 adjoining U.S. states, exclude the non-contiguous states of Alaska and Hawaii, District of Columbia and all off-shore insular areas) from 1975 to 2016. Section 4 presents the results of the analysis with the corresponding discussion. We conclude with recommendations and give further research directions in Section 5. Three tables in Appendix A shows the names of the lower states and the corresponding codes, as well as the detailed estimation results of SAR regressions.

2. Methodology

To explore the dynamics of fatality risk in the US lower states, a novel method for studying temporal instability and spatial distribution dynamics was employed. The traffic fatality risk was viewed from the lens of discrete Markov chains and the transitions of neighborhoods across levels of fatality risk over time.

2.1. Classic Markov chains

To define the data probability distribution, the starting point was the variable $r_{i,t}$, which represents the traffic fatality risk in the area, i, during the time period, t. This variable was classified into one of the K states. As suggested by Rey (2004), the state upper boundaries correspond to the quintile, s, of fatality risk over all lower states in a given time period, t. For example, if the state variable $x_{i,t} = j$, then $Q_{j-1,t} < r_{i,t} \leq Q_{j,t}$, where $Q_{j,t}$ is the quintile threshold for a period, t.

The core tenet of classic Markov chain modeling is to map the traffic fatality risk distribution from one period into the distribution for the next period, thus tracing out the evolution of the distribution over time. For this purpose, estimates of the probability transition matrix were obtained using the following formulation:

$$m_{j,1} = \frac{\sum_t n_{j,1,t}}{\sum_t \sum_m^K n_{j,m,t}} \tag{1}$$

where $n_{j,1,t}$ is the observed number of units that transitioned from traffic fatality state, j, to state 1 during the period (t, t+ 1). This value was obtained by:

$$n_{j,1,t} = \sum_r \gamma_{r,j,1,t} \tag{2}$$

where

$$\gamma_{r,j,1,t} = \begin{cases} 1 & if \;\; x_{i,t} = j \;\; and \;\; x_{i,t+1} = 1 \\ 0 & otherwise \end{cases} \tag{3}$$

Here, the chain was assumed to be temporally homogeneous, meaning the transition probabilities were time constant. The transition probability matrix consisted of K× K estimates according to:

$$M_{t,t+s} = \begin{pmatrix} m_{11} & \cdots & m_{1k} \\ m_{21} & \cdots & m_{2k} \\ \cdots & \cdots & \cdots \\ m_{k1} & \cdots & m_{kk} \end{pmatrix} \tag{4}$$

The process of fatality risk distribution from one period into the distribution for the next period can be denoted as:

$$P_{t+s} = P_t M_{t,t+s} \tag{5}$$

where P_t is a 1 × k probability distribution vector that summarizes the distribution for the period, t. Thus, a number of useful summary measures can then be derived from the transition probability matrix. As stated by a recent study (Clark and Rey, 2017), there are three conditions that the chain should obey: [1] irreducibility, means every state is reachable from every other state over time; [2] all states should be positive recurrent; and [3] homogeneity, i.e. the transition probabilities are time-invariant. Based on these conditions, the steady-state, or distribution of the chain can be estimated by:

$$\hat{\pi}_*' = \hat{\pi}_*' \hat{P} \tag{6}$$

such that:

$$\hat{\prod}_* = \hat{P}_{V \to \infty}^V \tag{7}$$

and:

$$\hat{\prod}_{i,j} = \hat{\prod}_{i+1,j} = \ldots = \hat{\prod}_{k,j}, \; \forall j \tag{8}$$

which implies that any row represents the transpose of the ergodic

distribution $\hat{\Pi}_*$.

Additionally, the first mean passage time required for the chain to pass from level j to level m is given as:

$$\hat{F} = (I - \hat{Z} + E\hat{Z})\hat{D} \tag{9}$$

where

$$\hat{Z} = (I - \hat{P} + \hat{\Pi})^{-1} \tag{10}$$

and E= ιι′ where ι is a vector of ones, and ι′ is its transpose, $\hat{D} = (\hat{\Pi})^{-1}$. When i= j, the first mean passage time was referred to as the recurrence time.

2.2. Spatial Markov chains

Whereas the classic discrete Markov chain is a flexible framework to model the transitional dynamics, there are some potential limitations on it when applied in a spatial context. A key assumption is that each spatial unit provides the time series of transitions information independently. However, this independence rule assumes that the changes of all analytic units were not influenced by their adjacent areas. To the extent that such interactions are at work, the role of spatial spillovers in the dynamics may be neglected by the classic discrete Markov chain.

One approach to extend the classic discrete Markov chain framework to appropriately account for the spatial effect is named spatial Markov chain, which was first proposed by Rey (2001). By estimating conditional transition probability matrices with the following elements, the spatial Markov chain provides a mechanism to allow the transition probabilities to be conditioned upon the spatial context of an area:

$$\hat{p}(s)_{j,1} = \frac{\sum_t n(s)_{j,1,t}}{\sum_t \sum_{m=1}^{K} n(s)_{j,m,t}} \tag{11}$$

where $n(s)_{j,1,t}$ is the observed number of areas that transitioned from state j to 1 over the period (t, t+ 1) and whose neighbors had fatality risks in state, s, in the period, t. The latter was determined by first using the spatial lag of fatality risks that were defined as: $\tilde{r}_{i,t} = \sum_b w_{i,b} r_{b,t}$, where $w_{i,b}$ is a spatial weight indicating the potential interaction between area i and b. Here, a row standardized contiguity matrix was used such that $w_{i,b} = \frac{c_{i,b}}{\sum_b c_{i,b}}$ where $c_{i,b} = 1$ if area i and b are neighboring areas. It was equal to 0 otherwise.

In a similar approach to the discretization of the original traffic fatality risk, $x_{i,t} = j$ equal to $Q_{j-1,t} < r_{i,t} \leq Q_{j,t}$. From this, the following values can be found out:

$$n(s)_{j,1,t} = \sum_r \Upsilon(s)_{r,j,1,t} \tag{12}$$

where

$$\gamma(s)_{r,j,1,t} = \begin{cases} 1 & if \;\; x_{i,t} = j \;\; and \;\; x_{i,t+1} = 1 \\ 0 & otherwise \end{cases} \tag{13}$$

and L is the lag operator.

2.3. Space-time interaction tests

2.3.1. Spatial correlation test

Moran's I was used to reflect whether, or not, observed fatality risks were spatially correlated among adjacent road entities (Aguero-Valverde and Jovanis, 2006):

$$I = {}^{n}\!/_{S_0} \sum_i \sum_b z_i w_{i,b} z_b / \sum_i z_i z_b \tag{14}$$

where $w_{i,b}$ is a spatial weight, $z_i = y_i - \bar{y}$, and $S_0 = \sum_i \sum_b w_{i,b}$. $\bar{y}$ is the global average of fatality risks in all observations.

2.3.2. Space-time interaction test

The estimation of K and K× K transition probability matrixes can be obtained by applying the spatial Markov chain, one for each state of the spatial lag. To examine whether it is necessary to consider the spatial effects, likelihood ratio (LR) and χ^2 tests of whether the probability transition matrixes are different across these levels were applied in this study. More formally:

$$\begin{aligned} H_0&: p(1)_{j,1} = p(2)_{j,1} = ... = p(K)_{j,1} = p_{j,1} \;\; \forall \, j, \, 1 \\ H_a&: \exists \; a: p(a)_{j,1} \neq p_{j,1} (k = 1, ..., K) \end{aligned} \tag{15}$$

Rejection of the null hypothesis in favor of the alternative, such that the transition probabilities are different, leads to the question of how the long-run dynamics of traffic fatality risks may be impacted by the neighborhood character. To answer this, estimates of the steady-state distribution and the first mean passage time can be obtained for each of the conditional chains from the estimated conditional probability transition matrix.

2.4. Spatial autoregressive models

In order to show the difference between the spatial Markov model and conventional spatial models in geography, the spatial autoregressive (SAR) model was chosen as the reference for comparison. The SAR model, which adds an explanatory variable in the form of a spatially lagged dependent variable, has been widely used in spatial economics analysis (Anselin, 1988). The basic formation of SAR models is given below:

$$y_i = \beta_0 + \lambda W y_i + \varepsilon_i \tag{16}$$

where y_i is an N× 1 vector of cross-sectional dependent variables for state i. Wy_i is the lag of the dependent variable for spatial weighted matrix W, and the 0–1 contiguous matrix W is the same setup as aforementioned in Section 2.2. Unlike many traditional econometric studies, the fatality rate data used in this study are panel data. Thus, the basic form of SAR models needs an update to fit the current datasets, the formation of SAR models with random effects for panel data are shown as follows:

$$y_{it} = \beta_0 + \lambda W y_{it} + \beta X_{it} + \varepsilon_i + \mu_{it} \tag{17}$$

$$\mu_{it} = \rho M \mu_{it} + \upsilon_{it} \tag{18}$$

where X_{it} is time-invariant regressors for time period t, in this study, X_{it} only contain the year to account for the temporal dynamics; ε_i are the random effects with mean 0 and variance σ_c^2; μ_{it} is an N× 1 vector of spatially lagged error; $\upsilon_{it} = (\upsilon_{1t}, \upsilon_{2t}, ..., \upsilon_{nt})'$ is an N× 1 vector of innovations (disturbances), and υ_{it} is independent and identically distributed across i and t with variance σ^2. W and M are the N× N spatial weighting matrices, and W is equal to M in this study.

By using the panel SAR models, the trend of fatality rate for different exposure can be analyzed in one explicit state across all U.S. lower states, which may lose key information and produce bias if there are different kinds of changing patterns.

3. Data description

Safety performance in one specific area can be evaluated by various safety indicators, such as the number of crashes, fatalities, or fatality risk. These indicators can be roughly categorized by their continuous and discrete nature. Compared to the discrete indicators (e.g., number of crashes or fatalities), the risk rate is more appealing because it naturally incorporates the effect of crash exposure, especially for the evaluation of road safety performance at areal levels (Zeng et al., 2017). As one of the most important safety indicators, the fatal risk is chosen to represent the safety states for state-level areas in this study. Moreover, previous studies have found that safety performance seems to differ according to the choice of exposure (Huang et al., 2010; Bouaoun et al.,

2015). Therefore, two kinds of exposures (i.e., vehicle miles and population) were employed in this study to make the conclusion more robust.

To explore the strength and duration of spatial effects for different exposures, this study used data from 1975 to 2015 from the 48 lower states in the United States. The measurement of interest was the level of traffic fatality risk, expressed as the mean number of traffic fatalities per 10,000 residents or per 100 million vehicle miles (VMs), which is a continuous measure bounded below by zero.

The traffic fatality number was extracted from the fatality analysis reporting system (FARS), which stores the data for all crash-related fatalities for the years 1975–2015. The FARS has collected fatal crash data for all 50 American states, Washington D.C., and Puerto Rico since 1975 (Lombardi et al., 2017). In order to incorporate the spatial dimension into this study, only the lower states were considered. The FARS data were obtained from various sources: police accident reports, death certificates, state vehicle registration files, coroner/medical examiner reports, state driver licensing files, hospital medical reports, state highway department data, and other state records. These data were gathered, transferred to the National Center for Statistics and Analysis and translated in a standard format by FARS state analysts. The victims' personal information is erased and the data are open-download to the public, which fully conforms to the Privacy Act from the National Highway Traffic Safety Administration (NHTSA) website.

As to risk exposure, VMs and population are frequently used exposure variables in safety analyses and government reports (Huang et al., 2010). The annual VMs of those states are obtained from the office of highway policy information at the Federal Highway Administration (2017). The FHWA stores abundant statistical data about the American highway system, including motor-fuel consumption, vehicle registration, and highway usage characteristics. The VM travel estimates are recorded in millions of miles by state and the statics are published annually. The annual population variation of every state can be found on the website of the U.S. Census Bureau (USCB) under the topic "population". The USCB provide the intercensal estimates of the population for various administrative divisions of the US between 1975 and 2015. At the beginning of every decade, a national census is conducted to investigate the population of each unit, and then the postcensal estimates are published on the Internet. In the year between two censuses, the USCB will provide the annual population estimates by adjusting the existing time series of postcensal estimates (National Center for Health Statistics, 2004). Moreover, it is worth noting that, to avoid the over-dispersion of data, the observations were transformed to relative fatality risks (by standardizing by each year by the mean).

The changes of fatality risks measured by the VMs and the population of the lower states are illustrated in Fig. 1, which shows there was a continuous decrease in the traffic fatality risk since the early 1980s. The decline of risk by VMs was sharper than for the population. However, traffic fatalities and fatality risks for either exposure rose in 2015 after a slight drop in 2013 and 2014, which highlights the challenges faced by safety policy-makers.

The traffic fatality risk measured by VMs and the population of all lower American states were used for this study. The geographic information system (GIS) was used to visualize the temporal and spatial dynamics of traffic fatality risk for these states. Figs. 2 and 3 show the maps for the level of traffic fatality risks for different exposures, $r_{i,t}$, for the census years 1975, 1995, 2005, and 2015 for both administrative divisions. The change in Fig. 2 is relatively more apparent than Fig. 3 since the fatality risk by VM for all states was at a relatively high level in the beginning.

The dynamics for the fatality risk for these administrative divisions are shown in Fig. 4, where the x-axis stands for the year and the y-axis represents the units that are coded by alphabetic order of their names (see Table A1 in Appendix). The color of the graph shows the traffic fatality risk levels for these administrative divisions, where red indicates a higher fatality risk and green indicates the opposite. It is clear that the traffic

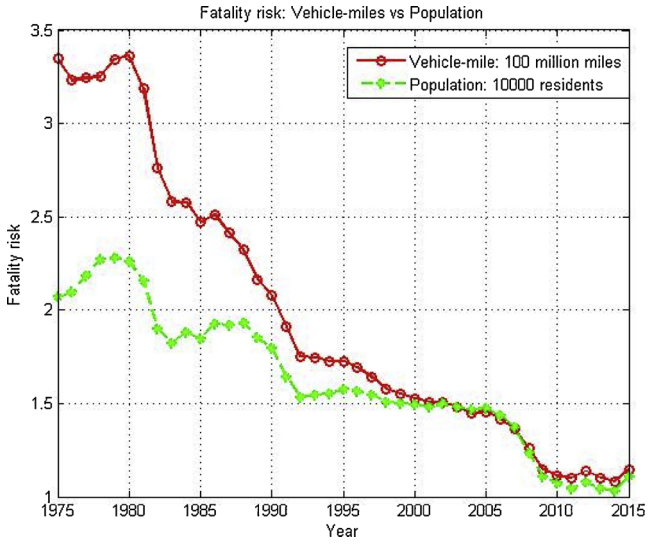

Fig. 1. Exposure comparison: vehicle miles vs. population.

fatality risks for these administrative divisions are likely to increase again if they have red records before in both administrative levels.

4. Results and discussion

With regards to model implementation, PySAL was used for the spatial dynamic analysis in this study because it can support a large and comprehensive standard library for spatial and temporal analysis (Rey and Anselin, 2007). Considering both the previous example (Rey, 2001) and the preconditions mentioned in Section 2.1, We can accordingly categorize the relative fatality risk into the following classes:

- Lowest quintile (q_1): the traffic fatality rate lying below the 80% mean value;
- Second lowest (q_2): the traffic fatality rate lying between 80% and 90% of the mean value;
- Middle quintile (q_3): the traffic fatality rate lying between 90% and 100% of the mean value;
- Second highest (q_4): the traffic fatality rate lying between 100% and 120% of the mean value;
- Highest quintile (q_5): the traffic fatality rate lying above 120% of the mean value.

Therefore, the five classes can be ordered as follows, from best to worst: $q_1 < q_2 < q_3 < q_4 < q_5$. The ascending order reflects the decrease in safety performance as we move from class to class.

4.1. Non-spatial results

For comparison purposes, the classic Markov chain model was also used to provide the non-spatial estimates. The transition matrix at the top of Table 1 shows the transition counts in the level of fatality risk, $\eta_{ij,t}$. For the VM and population cases, the sum of each matrix was the same at 1920. This is the number of risk states that the 48 states made from 1975 to 2015. Both matrices were diagonal with the number of transitions diminishing further from the diagonal.

As indicated by the counts for each level of fatality risk, the most likely outcome was that the state remained in the same quintile during the period of 1975–2015 for either administrative division. In order to understand the overall change pattern in the state-level fatality risk distribution, transition counts were translated into transition probabilities ($\hat{p}_{j,1}$) in the middle of Table 1.

As shown in the middle of Table 1, the fatality risk measured by VMs was more stationary than for the population because of the

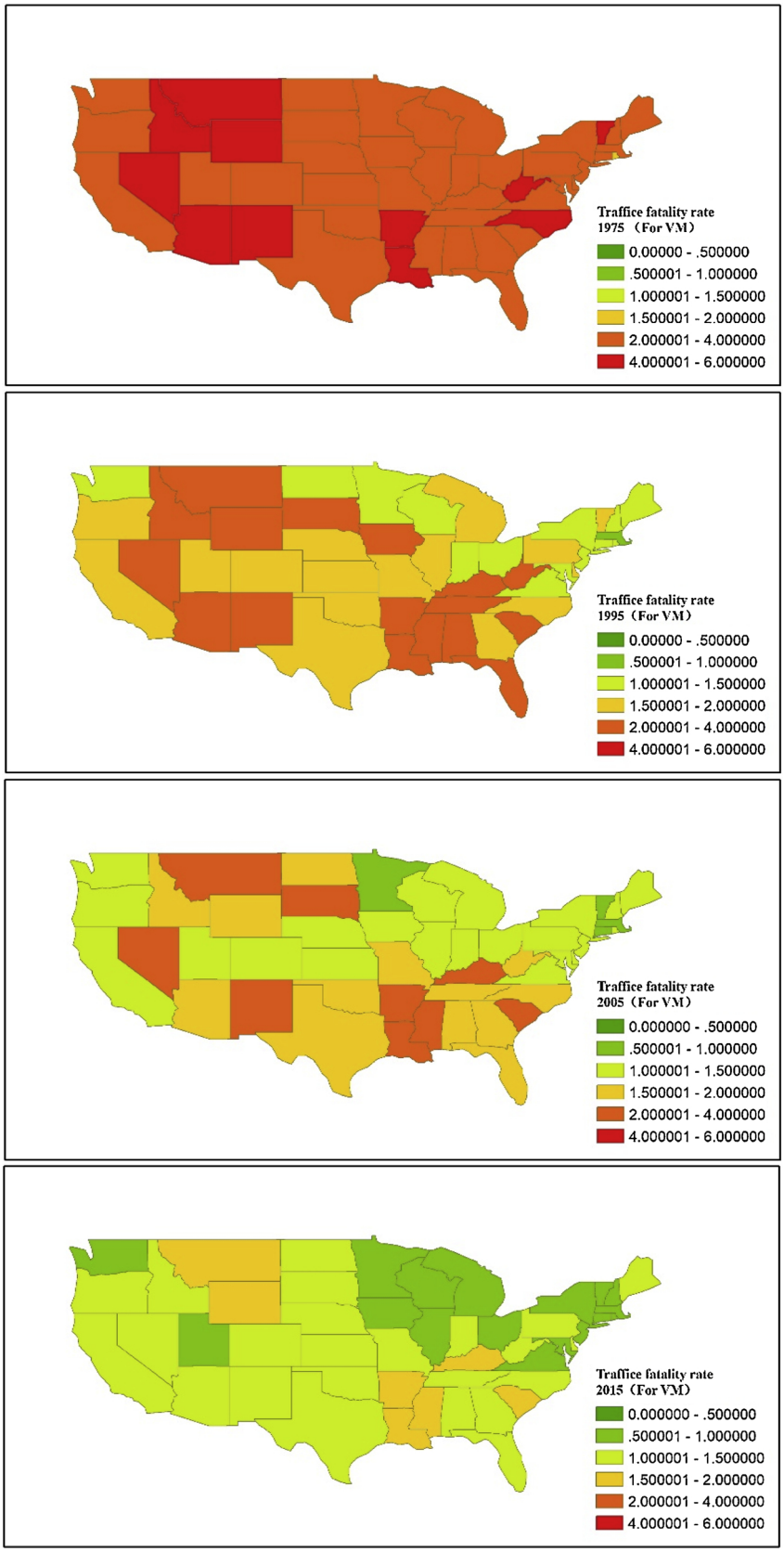

Fig. 2. Dynamic of fatality risk per 100 million VMs in the lower 48 American states for 1975, 1995, 2005, and 2015.

relatively large diagonal values. The steady-state probabilities ($\hat{\pi}_*'$) were slightly different but all close to 0.2 ($\hat{\pi}_1'$, $\hat{\pi}_2'$, $\hat{\pi}_3'$, $\hat{\pi}_4'$, $\hat{\pi}_5'$: 0.206, 0.195, 0.186, 0.201, 0.212 for VMs; 0.200, 0.187, 0.184, 0.202, 0.227 for population). The ergodic values for estimating the first mean passage time ($\hat{F}$) between traffic fatality risk levels are given at the bottom of Table 1.

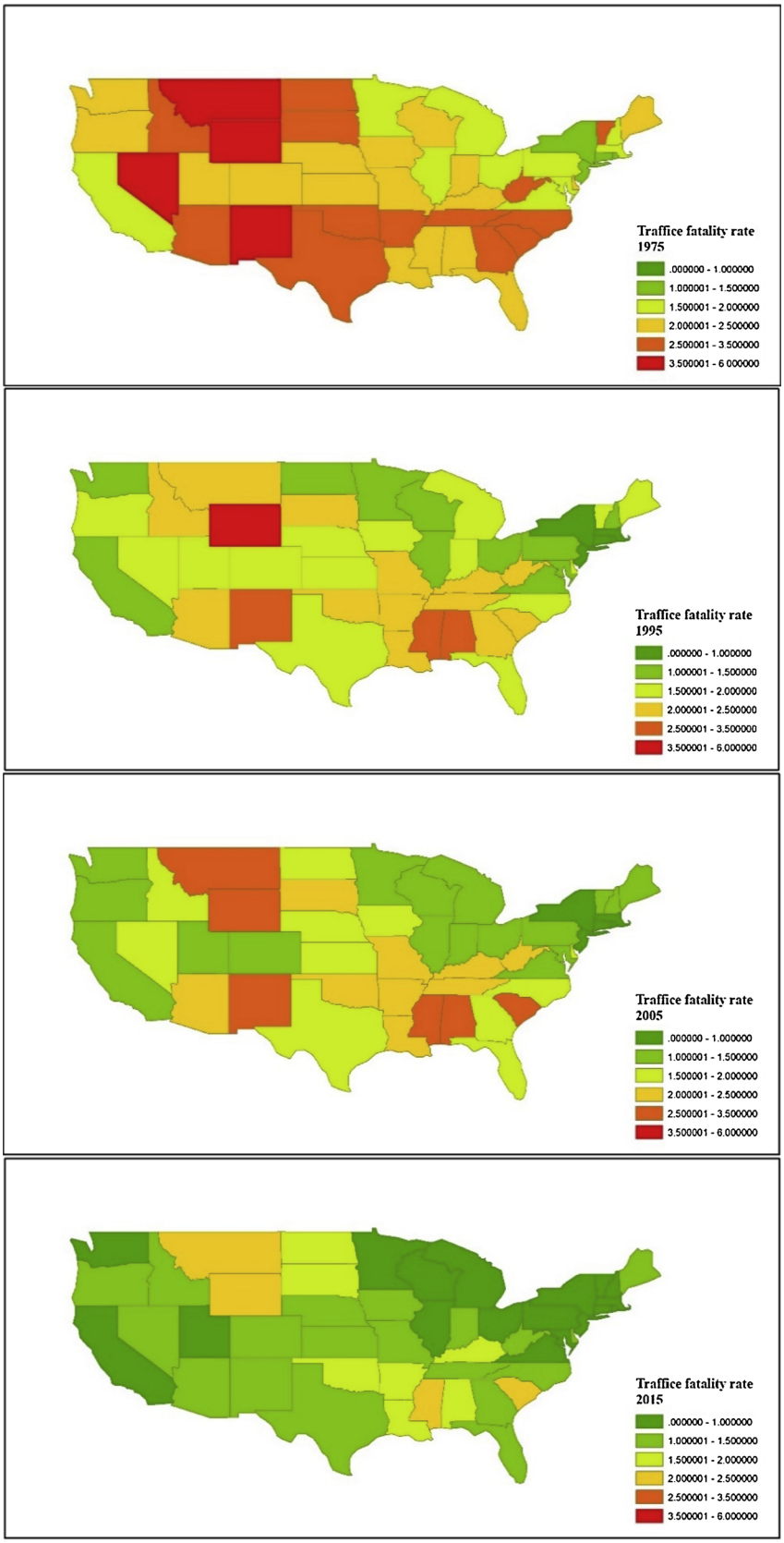

Fig. 3. Dynamic of fatality risk per 10,000 residents in the lower 48 American states for 1975, 1995, 2005, and 2015.

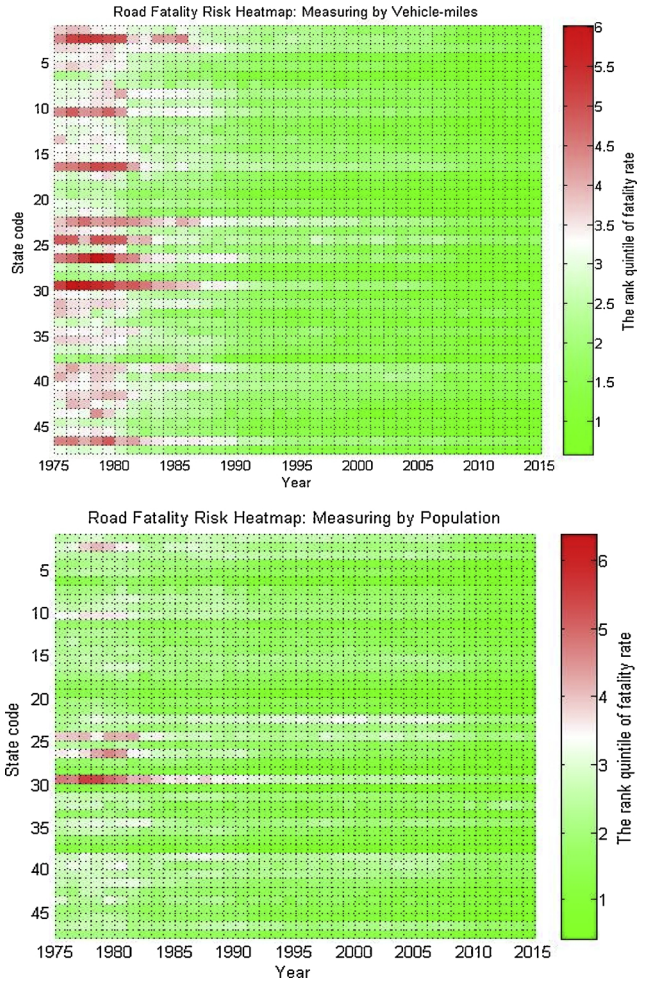

Fig. 4. Dynamic heat map for traffic fatality risks for different exposures.

As mentioned, the basic time unit of these passage periods was one year. Thus, in the VMs case, for a state with fatality risk in the first (lowest) quintile, it took about 6.07 years to enter the second quintile, 12.58 to get to the third quintile, 23.33 and 45.87 years to enter the fourth and fifth quintile respectively. With regard to the population case, the ($\hat{F}$) values were relatively longer than for the VMs case in the switching process. A state that started from the first quintile needed an average of 8.27, 17.36, 33.01, and 61.47 years to enter the second, third, fourth and fifth quintiles, respectively.

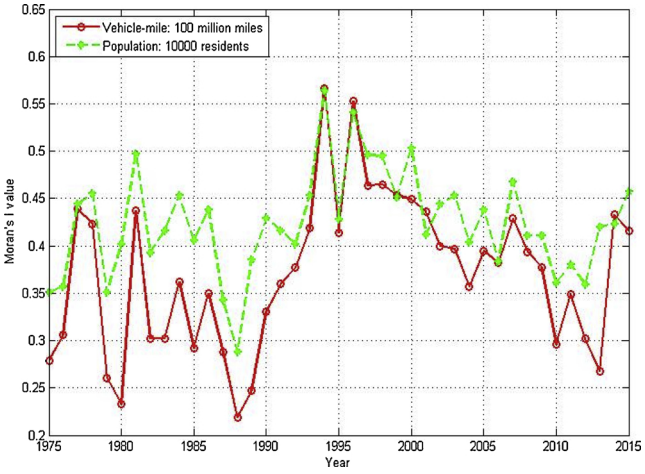

Fig. 5. The Moran's I values for fatal risks based on vehicle-miles and population.

4.2. Space-time interaction test results

Before showing the results for the spatial Markov chain model for these data, the degree of spatial correlation was tested. The Moran's I values for annual fatality risk are shown in Fig. 5, where the p-values of all state-level Moran's I values is less than 0.05, which indicated that the fatality risk levels for the lower states were spatially clustered at a 5% significance level. Fig. 5 also shows that the cluster levels for the population risk data are higher than those of the VMs, but both of their p-values support that the data used were clustered at the 95% confidence level during the whole period.

In Section 2.3, two types of statistic were introduced to test whether, or not, the probability transition matrices were different amongst the levels of fatality risks. The results of the tests are shown in Table 2. Both LR and χ^2 tests showed that p-values in both cases were significant at the 1% level (0.00), indicating that the transition probabilities were not homogeneous across the quintiles of fatality risk. The result

Table 1
Transition matrixes for VMs and population.

	By vehicle-miles					By population				
State level	(q_1)	(q_2)	(q_3)	(q_4)	(q_5)	(q_1)	(q_2)	(q_3)	(q_4)	(q_5)
	Transition Counts									
(q_1)	294	77	10	2	0	331	49	3	0	0
(q_2)	84	217	74	9	1	53	255	72	4	0
(q_3)	11	82	224	70	2	3	67	259	60	0
(q_4)	0	9	66	243	59	0	10	47	272	51
(q_5)	0	0	1	59	326	0	0	0	46	338
	Transition Probabilities									
(q_1)	0.768	0.201	0.026	0.005	0	0.864	0.128	0.008	0	0
(q_2)	0.218	0.564	0.192	0.023	0.003	0.138	0.664	0.188	0.010	0
(q_3)	0.028	0.211	0.576	0.180	0.005	0.008	0.172	0.666	0.154	0
(q_4)	0	0.024	0.175	0.645	0.156	0	0.026	0.124	0.716	0.134
(q_5)	0	0	0.003	0.153	0.845	0	0	0	0.120	0.880
	The first mean passage times for ergodic transition probability matrixes									
(q_1)	4.85	6.07	12.58	23.33	45.87	5.00	8.27	17.36	33.01	61.47
(q_2)	15.09	5.11	9.28	20.17	42.66	28.62	5.36	10.60	26.16	54.62
(q_3)	24.47	11.67	5.39	14.02	36.69	42.92	15.67	5.43	17.24	45.70
(q_4)	33.32	20.25	11.06	4.98	23.75	54.55	27.06	16.00	4.94	28.46
(q_5)	39.61	26.54	17.30	6.67	4.73	62.90	35.41	24.34	8.35	4.41

Table 2
The results of the Wilcoxon rank-based test for space-time intersection effects.

Test	By Vehicle miles (VMs)		By Population	
	LR	χ^2	LR	χ^2
Statistic value	168.959	227.729	154.352	293.924
P-value	.000	.000	.000	.000

illustrated the necessity of applying spatial Markov chain model to estimate the transition matrices and ergodic values.

4.3. Spatial results

The spatial extensions were used to estimate the spatial equivalents of the classic Markov chain results. The spatial equivalents of the transition probabilities were omitted in this paper because they reflected the similar feature to the spatially ergodic values matrix. Table 3 shows the estimated steady-state probabilities for each quintile. In contrast, the values for non-spatial cases are all at around 0.2.

In VMs case, the long-run distribution for states with surrounding neighbors that have levels of fatality risk in the lowest quintile is 59.0% to be in the lowest quintile, 24.0%, 12.4% and 3.7% in the second-lowest quintile, middle quintile and the second-highest quintile, respectively, and just 0.9% chance to become the highest quintile. For those states with neighbors in the highest quintile, just 3.9% are in the lowest quintile whereas 38.6% are in the highest quintile. As to the population case, when one state was surrounded by lowest quintile level neighbors, its probabilities to be in (q_1), (q_2), (q_3), (q_4) and (q_5) are 64.3%, 15.7%, 11.1%, 8.4% and 0.5%. In contrast, the probabilities of states surrounded by the highest quintile level neighbors were 3.7%, 6.8%, 12.7%, 28.6%, and 48.3%. To illustrate the spatial change trends, the spatial Markov ergodic estimate matrix was introduced in this section. As a modification of traditional Markov ergodic estimate matrix, the spatial Markov matrix was transformed from the traditional $k \times k$ matrix into a $k \times k \times k$ system. The spatial ergodic estimates are shown in Tables 4 and 5 and may be compared with the non-spatial equivalents in the matrix in Table 1.

The two sets of matrices show that transitions of a unit to a higher level of fatality risk are slower when its neighbors are at low levels but faster when the neighbors are at higher levels. In addition, it takes a longer time for a unit at a high level with higher-level neighbors to transit down, but a shorter time if the neighbors are at the lower levels. For example, in Table 1 for the VMs case, the first mean passage time for the lowest fatality risk states needs 6.07, 12.58, 23.33 and 45.87 years to become higher risk level ones. However, as illustrated in Table 4, the time requirements are extended to 5.88, 14.16, 37.59, and 166.89 years when the unit was surrounded by the lowest risk states and reduced to 3.00, 11.60, 10.14, 33.05 years when surrounded by the highest states. The overall change pattern in the fatality risks level based on population data is consistent with the risks based on VMs data, but the ergodic values are relatively larger when a state is located in neighborhoods with lowest fatality rate level. As shown in Table 5, it takes 11.81, 23.43, 28.09 and 378.69 years for the lowest level state surrounded by lowest risk neighbors to transit to four higher fatality risk levels. In terms of the lowest level states with highest risk level neighbors, it takes 14.26, 9.30, 9.24 and 25.30 years, on average, to rise to the second, third, fourth and fifth level of fatality risk, respectively. Obviously, in population case, compared to surrounding with the Lowest fatality rate, the state starting from the lowest risk level is more likely to become the worse situation than the second level of fatality rate when sitting in neighborhoods with the highest level of fatality rate.

Following the study of Agovino et al. (2019), for both exposures, we count all cases of states whose neighbors sit in better, same or worse traffic fatality rate classes respectively in Table 6. We also count the cases as well as their probabilities of safety state that improve, keep or worsen their classes, given that the state is surrounded by neighbors with a specified fatality rate level (better, similar or worse).

The calculations reported in Table 6 for two exposures show that: 1) if a unit is surrounded by neighbors with better (worse) fatality rate, it has a higher probability to improve (worsen) its fatality rate; 2) the probability of a state to keep in the starting traffic fatality rate level is relatively high, especially when it is surrounded by neighbors with the same fatality rate level; 3) the fatality risk levels by population are more likely to keep their original state, since the case counts whose level are

Table 4
The first mean passage time estimates of the spatial Markov chain model for the vehicle-miles.

Fatality risk level of surrounding neighbors	Starting state	First mean passage time				
		(q_1)	(q_2)	(q_3)	(q_4)	(q_5)
(q_1)	(q_1)	1.70	5.88	14.16	37.59	166.89
	(q_2)	3.40	4.17	11.00	33.05	162.91
	(q_3)	4.61	3.54	8.05	29.45	156.29
	(q_4)	4.25	4.17	10.24	27.06	143.01
	(q_5)	5.59	5.50	11.57	1.33	108.26
(q_2)	(q_1)	4.04	7.90	10.21	23.92	55.44
	(q_2)	15.29	3.20	5.54	23.33	54.85
	(q_3)	17.74	4.92	3.88	19.43	50.95
	(q_4)	21.60	8.04	6.26	11.45	31.52
	(q_5)	24.31	11.00	8.17	10.48	10.50
(q_3)	(q_1)	4.29	5.14	12.69	22.68	58.12
	(q_2)	14.87	3.86	8.55	18.43	53.87
	(q_3)	21.70	8.41	5.36	11.64	47.08
	(q_4)	26.79	13.32	6.85	4.45	35.44
	(q_5)	30.32	16.86	10.26	4.64	10.37
(q_4)	(q_1)	8.04	5.29	12.80	15.54	25.46
	(q_2)	19.48	8.38	10.24	13.25	23.11
	(q_3)	36.54	21.08	7.73	7.74	18.02
	(q_4)	46.54	32.50	15.31	3.37	11.08
	(q_5)	51.84	37.77	20.49	5.71	3.03
(q_5)	(q_1)	25.81	3.00	11.60	10.14	33.05
	(q_2)	74.42	15.48	8.60	7.14	30.05
	(q_3)	104.52	30.10	4.50	6.27	27.59
	(q_4)	113.73	39.31	9.21	3.47	24.51
	(q_5)	129.16	54.74	24.64	15.43	2.59

Table 3
The steady states distributions for the VMs and population.

State level	By vehicle-miles					By population				
	(q_1)	(q_2)	(q_3)	(q_4)	(q_5)	(q_1)	(q_2)	(q_3)	(q_4)	(q_5)
(q_1)	0.590	0.240	0.124	0.037	0.009	0.638	0.156	0.113	0.087	0.006
(q_2)	0.247	0.312	0.258	0.087	0.095	0.454	0.282	0.152	0.050	0.062
(q_3)	0.233	0.259	0.187	0.225	0.096	0.446	0.124	0.146	0.133	0.152
(q_4)	0.124	0.119	0.129	0.297	0.330	0.236	0.071	0.068	0.262	0.363
(q_5)	0.039	0.065	0.222	0.288	0.386	0.034	0.069	0.124	0.299	0.474

Table 5
The first mean passage time estimates of the spatial Markov chain model for the population.

Fatality risk level of surrounding neighbors	Starting state	First mean passage time				
		(q_1)	(q_2)	(q_3)	(q_4)	(q_5)
(q_1)	(q_1)	1.57	11.81	23.43	28.09	378.69
	(q_2)	5.54	6.40	15.09	20.07	370.36
	(q_3)	7.95	6.69	8.86	11.01	355.27
	(q_4)	7.60	5.34	11.80	11.43	367.07
	(q_5)	9.77	8.02	7.90	7.50	181.58
(q_2)	(q_1)	2.20	6.35	16.70	59.82	219.24
	(q_2)	5.66	3.55	13.74	56.86	216.29
	(q_3)	10.60	4.93	6.56	43.12	202.55
	(q_4)	16.02	10.36	5.43	19.99	159.43
	(q_5)	26.52	20.86	15.93	10.50	16.18
(q_3)	(q_1)	2.24	12.68	23.57	35.13	89.47
	(q_2)	12.80	8.08	14.23	25.38	79.73
	(q_3)	21.03	12.45	6.86	14.36	68.71
	(q_4)	26.43	17.50	7.27	7.54	54.34
	(q_5)	36.18	27.25	17.02	9.75	6.57
(q_4)	(q_1)	4.25	14.36	20.20	27.32	39.19
	(q_2)	26.82	14.06	12.94	19.64	31.51
	(q_3)	49.30	29.64	14.74	9.21	21.08
	(q_4)	60.66	45.48	28.85	3.81	11.87
	(q_5)	67.43	52.25	35.62	6.77	2.75
(q_5)	(q_1)	29.80	14.26	9.30	9.24	25.30
	(q_2)	90.10	14.59	9.83	6.51	22.57
	(q_3)	109.62	27.14	8.05	4.83	20.89
	(q_4)	123.96	40.28	18.97	3.34	16.06
	(q_5)	138.46	54.78	33.47	14.50	2.11

Table 6
Summary of spatial Markov chains analysis.

Transaction probabilities with better neighbors	Got worse	Got better	Stayed steady
By vehicle-miles	7.97% (47/590)	28.14% (166/590)	63.90% (377/590)
By population	9.40% (49/521)	24.18% (126/521)	66.41% (346/521)
Transaction probabilities with same neighbors	Got worse	Got better	Stayed steady
By vehicle-miles	17.62% (117/664)	10.99% (73/664)	71.39% (474/664)
By population	10.81% (85/786)	7.12% (56/786)	82.06% (627/786)
Transaction probabilities with worse neighbors	Got worse	Got better	Stayed steady
By vehicle-miles	24.02% (160/666)	13.66% (91/666)	62.31% (415/666)
By population	18.76% (115/613)	10.28% (63/613)	70.96% (435/613)

Note: case counts in the brackets.

stayed steady is smaller compared to population in VMs case (Table 6, *Stayed steady* column: 1266 vs. 1408). In summary, the neighbors may cause a phenomenon known as the "drag effect" that inhibits the movement of a state away from the surrounding neighborhood level of fatality risk (Clark and Rey, 2017).

4.4. Results of panel spatial autoregressive models

Since there are no other exploratory factors, the random effect panel models were applied in this study to account for the unobserved heterogeneity (Mothafer et al., 2017). The spatial lag, the standard deviation (SD) of panel effects, and the SD of the errors are shown in Table 7.

Table 7
The estimated coefficients on spatial lag, SD of panel effects and SD of errors.

	For VMs			For population		
	Mean	95% CI		Mean	95% CI	
Spatial lag	0.1669	0.1000	0.2337	0.0805	0.0141	0.1468
SD of panel effects	0.0043	0.0035	0.0052	0.5429	0.4439	0.6642
SD of errors	0.0029	0.0028	0.0030	0.2785	0.2698	0.2875

The estimated coefficients on the spatial lag of dependent variable are -0.16 and -0.08 respectively, indicating a significantly positive correlation between the traffic fatality rate in one state and the traffic fatality rate in a neighboring state. Moreover, the significance of the SD of panel effects and errors also indicates the necessity of applying the panel SAR model with random effects.

In order to present the temporal dynamics of different years, the dummy variables were created and the year 1975 was set as the reference. The mean and boundary of 95% confidence interval (CI) of these dummy years coefficients were shown in the following line charts (the details of regression results were added in the Appendix A Table B1 and Table C1).

The two charts in Fig. 6 show that the temporal effects of fatality rate changes are similar to the changes of fatality risks shown in the Fig. 1 and there are continuous downtrends for both exposures since 1980. However, as these yearly coefficients can only reflect the overall changes of fatality rate, the states of which transferring pattern against the dominant trend may not be reflected in the panel SAR models. In contrast, the spatial Markov model can better summarize the changing pattern of fatality rates since the different transiting patterns can also be counted in the transition matrix no matter how rare they are.

5. Conclusion

The time series technologies examining safety indicators rarely take the potential influence of surrounding neighborhoods into account. If this effect of spatial proximity is real but ignored, such transition trends would be ill-specified and the estimate results may be inefficient and biased. This study therefore applied a novel method to quantify the repeated cross-sectional extent of the influence from such neighborhoods and also capture the temporal strength over a 40-year time span. The key findings and contributions of this study are as follows: (i) a comparison of the steady-state probabilities and transition times in the

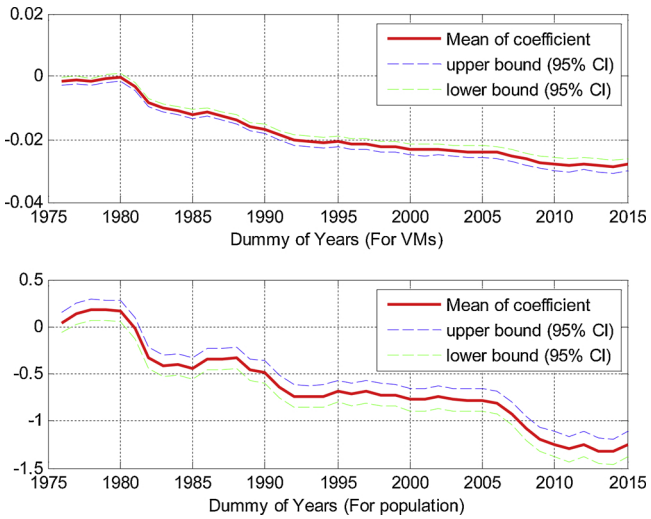

Fig. 6. The estimated coefficients on dummy years based on vehicle-miles (top chart) and population (bottom chart).

non-spatial and spatial cases obviously demonstrated the importance of considering influence of neighborhood context when modeling the transition of fatality risk, (ii) the duration to transition between the different levels of fatality risk was relatively long when the neighborhood context was different from that at the end of the transition, (iii) the incorporation of spatial effects into models was therefore likely to produce substantially different estimates and conclusions, and (iv) the influences of neighborhood were shown to be present, at least based on the exposure indictors for each state in the United States (i.e., VMs and population). Moreover, the presentation of panel spatial autoregressive model has proven the importance of using Markov chains models since the multiple state assumption in Markov chains model can help to better account for the changing pattern occurred with low probability (i.e. against the overall trend).

In the context of the existing literature, this is one of the first studies estimating the strength of the spatial relationships in traffic fatality risks over time using aggregate data. The aggregate nature of the data provides a broader understanding of state-level fatality risk than the partial picture obtained from sparser disaggregate data. The time span of this study is long enough (40 years), during which the traffic fatality rate experienced periods of relative stability, rapid growth, and decline, thereby allowing us to provide estimates that are not influenced by the short-term random fluctuation that some individual panel data may capture. This paper also provides a new perspective to the acquisition, explanation, and forecast of fatality risk's variation trend for an administrative division.

In terms of policyimplication, the finding of this study is also fairly informative, especially for long-term road safety policies influenced by traffic fatality risks. A neighborhood at relatively low levels of fatality risk is more likely to remain the status if it is surrounded by similar neighborhoods with low fatality risk but has a higher probability of transition to a higher level if surrounded by neighbors with higher levels of fatality risk. Thus, when allocating resources to improve safety performance, the government should take the safety trend of the neighborhood regions into consideration. Attention should be specifically paid to areas with neighbors at higher traffic fatality level and take measures to prevent crash deteriorations in advance. From the exposure perspective, the patterns of fatality risk measured by VMs and population are similar but the fatality risk measured by population is more stationary than that by VMs, implying that the safety indicator classification measured by the population may be less time-sensitive than that measured by the VMs.

Some interesting extensions to this work are worth exploring in future research. First, the issues related to the sensitivity of the metrics could be explored, which guide the choice of class numbers. The second extension would be to add more relative variables to the model for exploration of the relationship between risk factors and fatality risk. Moreover, the spatial dynamics were only tested within 48 American states, so more studies from other countries and regions would be expected to enhance our findings.

Declaration of Competing Interest

The authors declare that they have no known competing financial interests or personal relationships that could have appeared to influence the work reported in this paper.

Acknowledgment

This work was jointly supported by: 1) the Joint Research Scheme of National Natural Science Foundation of China/Research Grants Council of Hong Kong (Project No. 71561167001 & N_HKU707/15), 2) National Key Research and Development Plan (No. SQ2018YFB120181).

Appendix A

Table A1
Lower state names and their corresponding codes.

State name	Code	State name	Code	State name	Code	State name	Code	State name	Code	State name	Code
Alabama	1	Georgia	9	Maine	17	Nebraska	25	Ohio	33	Texas	41
Arizona	2	Idaho	10	Maryland	18	Nevada	26	Oklahoma	34	Utah	42
Arkansas	3	Illinois	11	Massachusetts	19	New Hampshire	27	Oregon	35	Vermont	43
California	4	Indiana	12	Michigan	20	New Jersey	28	Pennsylvania	36	Virginia	44
Colorado	5	Iowa	13	Minnesota	21	New Mexico	29	Rhode Island	37	Washington	45
Connecticut	6	Kansas	14	Mississippi	22	New York	30	South Carolina	38	West Virginia	46
Delaware	7	Kentucky	15	Missouri	23	North Carolina	31	South Dakota	39	Wisconsin	47
Florida	8	Louisiana	16	Montana	24	North Dakota	32	Tennessee	40	Wyoming	48

Table B1
The intercept and coefficients of dummy years for VMs.

Year	Mean	Std. Err.	p-value	95% confidence interval	
1976	−0.0014	0.0006	0.015	−0.0026	−0.0003
1977	−0.0011	0.0006	0.051	−0.0023	0.0000
1978	−0.0017	0.0006	0.004	−0.0028	−0.0005
1979	−0.0006	0.0006	0.34	−0.0017	0.0006
1980	−0.0001	0.0006	0.809	−0.0013	0.0010
1981	−0.0031	0.0006	0	−0.0043	−0.0020
1982	−0.0081	0.0006	0	−0.0094	−0.0069
1983	−0.0101	0.0007	0	−0.0114	−0.0088
1984	−0.0107	0.0007	0	−0.0120	−0.0094
1985	−0.0119	0.0007	0	−0.0133	−0.0106
1986	−0.0112	0.0007	0	−0.0125	−0.0099
1987	−0.0127	0.0007	0	−0.0140	−0.0113
1988	−0.0136	0.0007	0	−0.0150	−0.0123
1989	−0.0159	0.0007	0	−0.0174	−0.0145

(*continued on next page*)

Table B1 (*continued*)

Year	Mean	Std. Err.	p-value	95% confidence interval	
1990	−0.0168	0.0008	0	−0.0183	−0.0153
1991	−0.0186	0.0008	0	−0.0201	−0.0170
1992	−0.0203	0.0008	0	−0.0219	−0.0186
1993	−0.0206	0.0008	0	−0.0222	−0.0190
1994	−0.0210	0.0008	0	−0.0226	−0.0193
1995	−0.0207	0.0008	0	−0.0224	−0.0191
1996	−0.0214	0.0009	0	−0.0230	−0.0197
1997	−0.0215	0.0009	0	−0.0231	−0.0198
1998	−0.0222	0.0009	0	−0.0239	−0.0205
1999	−0.0225	0.0009	0	−0.0242	−0.0208
2000	−0.0231	0.0009	0	−0.0248	−0.0213
2001	−0.0234	0.0009	0	−0.0251	−0.0216
2002	−0.0232	0.0009	0	−0.0250	−0.0215
2003	−0.0235	0.0009	0	−0.0253	−0.0218
2004	−0.0239	0.0009	0	−0.0256	−0.0221
2005	−0.0239	0.0009	0	−0.0256	−0.0221
2006	−0.0242	0.0009	0	−0.0260	−0.0224
2007	−0.0252	0.0009	0	−0.0270	−0.0233
2008	−0.0264	0.0010	0	−0.0283	−0.0245
2009	−0.0274	0.0010	0	−0.0293	−0.0254
2010	−0.0278	0.0010	0	−0.0298	−0.0259
2011	−0.0283	0.0010	0	−0.0303	−0.0263
2012	−0.0278	0.0010	0	−0.0297	−0.0258
2013	−0.0284	0.0010	0	−0.0303	−0.0264
2014	−0.0287	0.0010	0	−0.0306	−0.0267
2015	−0.0280	0.0010	0	−0.0300	−0.0260
Constant	0.0416	0.0014	0	0.0388	0.0444

Table C1
The intercept and coefficients of dummy years for population.

Year	Mean	Std. Err.	p-value	95% confidence interval	
1976	0.0449	0.0569	0.43	−0.0665	0.1564
1977	0.1415	0.0570	0.013	0.0298	0.2532
1978	0.1843	0.0571	0.001	0.0723	0.2962
1979	0.1739	0.0571	0.002	0.0619	0.2859
1980	0.1628	0.0571	0.004	0.0508	0.2747
1981	−0.0212	0.0569	0.709	−0.1327	0.0902
1982	−0.3286	0.0577	0	−0.4416	−0.2155
1983	−0.4144	0.0582	0	−0.5286	−0.3003
1984	−0.4009	0.0580	0	−0.5147	−0.2871
1985	−0.4457	0.0583	0	−0.5600	−0.3314
1986	−0.3441	0.0578	0	−0.4573	−0.2309
1987	−0.3470	0.0578	0	−0.4602	−0.2337
1988	−0.3336	0.0577	0	−0.4467	−0.2206
1989	−0.4554	0.0585	0	−0.5701	−0.3407
1990	−0.4792	0.0588	0	−0.5944	−0.3640
1991	−0.6370	0.0601	0	−0.7548	−0.5191
1992	−0.7379	0.0612	0	−0.8579	−0.6179
1993	−0.7406	0.0612	0	−0.8604	−0.6207
1994	−0.7385	0.0613	0	−0.8586	−0.6185
1995	−0.6827	0.0606	0	−0.8014	−0.5639
1996	−0.7146	0.0609	0	−0.8339	−0.5953
1997	−0.6892	0.0607	0	−0.8081	−0.5702
1998	−0.7252	0.0609	0	−0.8446	−0.6058
1999	−0.7275	0.0610	0	−0.8471	−0.6078
2000	−0.7740	0.0617	0	−0.8948	−0.6531
2001	−0.7764	0.0616	0	−0.8972	−0.6555
2002	−0.7477	0.0614	0	−0.8679	−0.6274
2003	−0.7740	0.0618	0	−0.8950	−0.6529
2004	−0.7790	0.0618	0	−0.9001	−0.6580
2005	−0.7827	0.0619	0	−0.9040	−0.6614
2006	−0.8050	0.0622	0	−0.9269	−0.6832
2007	−0.9195	0.0637	0	−1.0443	−0.7947
2008	−1.0825	0.0660	0	−1.2118	−0.9532
2009	−1.1946	0.0679	0	−1.3276	−1.0616
2010	−1.2457	0.0687	0	−1.3803	−1.1110
2011	−1.2980	0.0698	0	−1.4349	−1.1611
2012	−1.2483	0.0688	0	−1.3831	−1.1134
2013	−1.3167	0.0700	0	−1.4540	−1.1795
2014	−1.3291	0.0702	0	−1.4667	−1.1914
2015	−1.2476	0.0687	0	−1.3822	−1.1129
Constant	2.5907	0.1192	0	2.3571	2.8244

References

Abdel-Aty, M., Lee, J., Siddiqui, C., Choi, K., 2013. Geographical unit based analysis in the context of transportation safety planning. Transp. Res. Part A Policy Pract. 49 (49), 62–75.

Agovino, M., Crociata, A., Sacco, P.L., 2019. Proximity effects in obesity rates in the US: a spatial Markov chains approach. Soc. Sci. Med. 220, 301–311.

Aguero-Valverde, J., Jovanis, P.P., 2006. Spatial analysis of fatal and injury crashes in Pennsylvania. Accid. Anal. Prev. 38 (3), 618–625.

Ahangari, H., Atkinson-Palombo, C., Garrick, N.W., 2016. Progress towards zero, an international comparison: improvements in traffic fatality from 1990 to 2010 for different age groups in the USA and 15 of its peers. J. Safety Res. 57, 61–70.

Anselin, L., 1988. Spatial Econometrics: Methods and Models. Kluwer Academic Publishers, Dordrecht.

Bergel-Hayat, R., Debbarh, M., Antoniou, C., Yannis, G., 2013. Explaining the road accident risk: weather effects. Accid. Anal. Prev. 60 (12), 456–465.

Boroujerdian, A.M., Saffarzadeh, M., Yousefi, H., Ghassemian, H., 2014. A model to identify high crash road segments with the dynamic segmentation method. Accid. Anal. Prev. 73, 274–287.

Bouaoun, L., Haddak, M.M., Amoros, E., 2015. Road crash fatality rates in France: a comparison of road user types, taking account of travel practices. Accid. Anal. Prev. 75, 217–225.

Bougueroua, M., Carnis, L., 2016. Economic development, mobility and traffic accidents in Algeria. Accid. Anal. Prev. 92, 168–174.

Clark, S.D., Rey, S., 2017. Temporal dynamics in local vehicle ownership for Great Britain. J. Transp. Geogr. 62, 30–37.

Commandeur, J.J., Bijleveld, F.D., Bergelhayat, R., Antoniou, C., Yannis, G., Papadimitriou, E., 2013. On statistical inference in time series analysis of the evolution of road safety. Accid. Anal. Prev. 60 (12), 424–434.

Dong, N., Huang, H., Lee, J., Gao, M., Abdel-Aty, M., 2016. Macroscopic hotspots identification: a Bayesian spatio-temporal interaction approach. Accid. Anal. Prev. 92, 256–264.

Federal Highway Administration, 2017. Highway Statistics Series (1975-2015). Available at policy and governmental affairs, Washington DC Accessed March 31, 2018. https://www.fhwa.dot.gov/policyinformation/statistics.cfm.

Gubner, J.A., 2006. Probability and Random Processes for Electrical and Computer Engineers. Cambridge University Press.

Huang, H., Abdel-Aty, M., Darwiche, A.L., 2010. County-level crash risk analysis in Florida. Transportation Research Record Journal of the Transportation Research Board 2148 (2148), 27–37.

Huang, H., Zhou, H., Wang, J., Chang, F., Ma, M., 2017. A multivariate spatial model of crash frequency by transportation modes for urban intersections. Anal. Methods Accid. Res. 14, 10–21.

Ko, J., Guensler, R., 2004. Application of the GARCH model for depicting a driver acceleration behavior on freeways. The CD-ROM Proceedings of the 81st Annual Meeting of the Transportation Research Board.

Lavrenz, S.M., Vlahogianni, E.I., Gkritza, K., Ke, Y., 2018. Time series modeling in traffic safety research. Accid. Anal. Prev. 368–380.

Lee, J., Abdel-Aty, M., Jiang, X., 2015. Multivariate crash modeling for motor vehicle and non-motorized modes at the macroscopic level. Accid. Anal. Prev. 78, 146–154.

Li, X., Wu, L., Yang, X., 2018. Exploring the impact of social economic variables on traffic safety performance in Hong Kong: a time series analysis. Saf. Sci. 109, 67–75.

Liu, C., Sharma, A., 2017. Exploring spatio-temporal effects in traffic crash trend analysis. Anal. Methods Accid. Res. 16, 104–116.

Liu, C., Sharma, A., 2018. Using the multivariate spatio-temporal Bayesian model to analyze traffic crashes by severity. Anal. Methods Accid. Res. 17, 14–31.

Lombardi, D.A., Horrey, W.J., Courtney, T.K., 2017. Age-related differences in fatal intersection crashes in the United States. Accid. Anal. Prev. 99, 20–29.

Loo, B.P., Anderson, T.K., 2015. Spatial Analysis Methods of Road Traffic Collisions. CRC Press.

Malyshkina, N.V., Mannering, F.L., 2009. Markov switching multinomial logit model: an application to accident-injury severities. Accid. Anal. Prev. 41 (4), 829–838.

Malyshkina, N.V., Mannering, F.L., Tarko, A.P., 2009. Markov switching negative binomial models: an application to vehicle accident frequencies. Accid. Anal. Prev. 41 (2), 217–226.

Meng, F., Xu, P., Wong, S.C., Huang, H., Li, Y.C., 2017. Occupant-level injury severity analyses for taxis in Hong Kong: a Bayesian space-time logitstic model. Accid. Anal. Prev. 108, 297–307.

Mothafer, G.I., Yamamoto, T., Shankar, V.N., 2017. A negative binomial crash sum model for time invariant heterogeneity in panel crash data: some insights. Anal. Methods Accid. Res. 14, 1–9.

National Center for Health Statistics, 2004. Bridged-race Intercensal Estimates of the July 1, 1990-July 1, 1999, United States Resident Population by County, Single-year of Age, Sex, Race, and Hispanic Origin, Prepared by the US Census Bureau With Support From the National Cancer institute. US Census Bureau with support from the National Cancer Institute, Washington, DC.

Noland, R.B., 2003. Traffic fatalities and injuries: the effect of changes in infrastructure and other trends. Accid. Anal. Prev. 35 (4), 599–611.

Park, B.J., Lord, D., 2009. Application of finite mixture models for vehicle crash data analysis. Accid. Anal. Prev. 41 (4), 683–691.

Quddus, M.A., 2008. Time series count data models: an empirical application to traffic accidents. Accid. Anal. Prev. 40 (5), 1732–1741.

Rey, S.J., 2001. Spatial empirics for economic growth and convergence. Geogr. Anal. 33 (3), 195–214.

Rey, S.J., 2004. Spatial dependence in the evolution of regional income distributions. Spatial econometrics and spatial statistics 194–213.

Rey, S.J., Anselin, L., 2007. PySAL: a Python library of spatial analytical methods. Rev. Reg. Stud. 37, 5–27.

Sebego, M., Naumann, R.B., Rudd, R.A., Voetsch, K., Dellinger, A.M., Ndlovu, C., 2014. The impact of alcohol and road traffic policies on crash rates in Botswana, 2004-2011: a time-series analysis. Accid. Anal. Prev. 70 (6), 33–39.

Truong, L.T., Kieu, L.M., Vu, T.A., 2016. Spatiotemporal and random parameter panel data models of traffic crash fatalities in Vietnam. Accid. Anal. Prev. 94, 153–161.

Wang, C., Quddus, M., Ryley, T., Enoch, M., Davison, L., 2012. Spatial models in transport: a review and assessment of methodological issues. Meeting of the Transportation Research Board.

World Health Organization, 2015. Global Status Report on Road Safety 2015. Geneva, Switzerland. .

Xu, P., Huang, H., Dong, N., Abdel-Aty, M., 2014. Sensitivity analysis in the context of regional safety modeling: identifying and assessing the modifiable areal unit problem. Accid. Anal. Prev. 70, 110–120.

Xu, P., Huang, H., 2015. Modeling crash spatial heterogeneity: random parameter versus geographically weighting. Accid. Anal. Prev. 75, 16–25.

Xu, P., Huang, H., Dong, N., Wong, S.C., 2017. Revisiting crash spatial heterogeneity: a Bayesian spatially varying coefficients approach. Accid. Anal. Prev. 98, 330–337.

Xu, P., Dong, N., Wong, S.C., Huang, H., 2019. Cyclists injured in traffic crashes in Hong Kong: a call for action. PLoS One 14 (8), e0220785.

Zeng, Q., Huang, H., 2014. Bayesian spatial joint modeling of traffic crashes on an urban road network. Accid. Anal. Prev. 67 (6), 105–112.

Zeng, Q., Wen, H., Huang, H., Abdel-Aty, M., 2017. A Bayesian spatial random parameters Tobit model for analyzing crash rates on roadway segments. Accid. Anal. Prev. 100, 37–43.